Characterization of a Ladder Polymer by Small-Angle X-ray and Neutron Scattering

P. Hickl and M. Ballauff*

Polymer-Institut, Universität Karlsruhe, Kaiserstrasse 12, 76128 Karlsruhe, Germany

U. Scherf and K. Müllen

Max-Planck-Institut für Polymerforschung, Ackermannweg 10, 55021 Mainz, Germany

P. Lindner

Institut Laue-Langevin, BP 156X, 38042 Grenoble, France

Received July 16, 1996; Revised Manuscript Received October 14, 1996[⊗]

ABSTRACT: An analysis of the conformation of a ribbon-type polymer in dilute solution is given. By combination of small-angle neutron scattering (SANS) and small-angle X-ray scattering (SAXS) the effect of the finite dimensions of the repeating units can be assessed separately. It is thus possible to evaluate the experimental data to yield the form factor of the corresponding infinitely thin chain. This form factor could be evaluated for three samples differing in molecular weight and compared to the theoretical expression furnished by Kholodenko (*Macromolecules* **1993**, *26*, 4179). Good agreement for all molecular weights under consideration here could be achieved. The analysis shows that the ribbon-type polymers under consideration here are wormlike chains with a persistence length of 6.5 nm.

Introduction

The synthesis of ladder polymers represents a considerable challenge to preparative polymer chemistry despite decades of research in this field. Some time ago, the first successful synthesis of a soluble and structurally well-defined poly(*p*-phenylene) ladder polymer LPPP possessing the structure was reported.[1,2] The synthetic

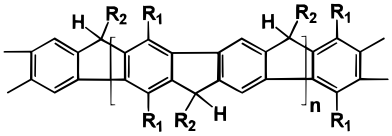

LPPP

R_1: -C_6H_{13}
R_2: -1,4-C_6H_4-$C_{10}H_{21}$

procedure leading to this novel type of ribbon-like structure followed the classical two-step route: A single stranded stiff-chain polymer which is suitably functionalized is cyclized in a second step by a polymer-analogous reaction. The good solubility of the ladder polymer allowed a comprehensive analysis by NMR which proved that the polymer-analogous reaction proceeded quantitatively. The polymer LPPP and related structures exhibit a highly efficient electroluminescence[3,4] which renders these materials interesting for the fabrication of light-emitting diodes.

A necessary prerequisite for electronic applications is the attainment of sufficiently high molecular weights to allow the production of free standing films. Previous investigations using gel-permation chromatography (GPC) had demonstrated indeed that high molecular weights of the ladder polymer LPPP can be achieved.[5] Another point of interest is the conformation of such a ladder-like macromolecule in solution. A number of studies[6−10] conducted on single-stranded stiff-chain polymers has demonstrated that these structure are characterized by rather low persistence lengths which are of the order of 5−15 nm. It is thus interesting to investigate the effect of the two-dimensional ribbon-type structure on the shape of the chains in solution.

In this paper we report a comprehensive study of conformation of the polymer LPPP in solution. By an investigation combining small-angle X-ray scattering[11] (SAXS) and small-angle neutron scattering[12] (SANS) the form factor $P(q)$ (q, magnitude of scattering vector; $q = (4\pi/\lambda)\sin(\theta/2)$; λ, wavelength of radiation, θ, scattering angle) of the chains could be determined and compared to theoretical models.

The use of different radiations turned out to be necessary to come to unambiguous conclusions with regard to conformation in solution. In general, statistical-mechanical models[12] of chain conformation are capable of furnishing the form factor termed $P_0(q)$ for an infinitely thin thread. Hence, $P_0(q)$ takes only into account interference from repeating units located at different positions along the chain; i.e., the repeating units are treated as pointlike scattering units. This assumption is fully justified when only looking at the region of smallest angles by, e.g., static light scattering. As shown in the course of a fundamental study by Rawiso, Duplessix, and Picot,[13] however, the effect of the finite diameter of the chains may alter considerably the scattering intensity of the chains at high q. Using partially deuterated polystyrene samples, these authors were able to discuss in a concise manner the effects of finite diameter, chain stiffness, and excluded volume on the scattering behavior of flexible chains in good solvents.

A previous study[14] of the poly(2,5-di-*n*-alkoxy-1,4-phenylene terephthalate)s by SANS corroborated this result. These polyesters present a stiff-chain polymer substituted by alkyl side chains similar to the structure of the LPPP. The analysis of these materials has shown as well that the effect of the finite lateral extensions will markedly alter the scattering curves in the region of higher scattering angles. It is therefore evident that this effect must be taken into account.

[⊗] Abstract published in *Advance ACS Abstracts,* January 1, 1997.

S0024-9297(96)01038-8 CCC: $14.00

Table 1. Characterization of the LPPP by SANS and SAXS

symbol		M_w (g/mol)	R_g (nm)	A^2 (mol·cm^3·g^{-2})	P_w[a]	R_c^2 (nm)	M_L [(g/mol)·nm]	L_w (nm)	M_w/M_n[b]	R_g[c] (nm)
LPPP-24	SAXS	25 000	7.8	9.0×10^{-4}	31	−0.19	835	29.8	2.0	8.0
	SANS	30 000	7.9	6.5×10^{-4}	37	0.64	1036	29.0	2.0	7.9
LPPP-50	SAXS	38 000	9.3	6.7×10^{-4}	47	−0.24	907	41.9	1.5	9.5
	SANS					0.62				
LPPP-99	SAXS									
	SANS	87 000	14.7	6.2×10^{-4}	110	0.70	1040	84.6	1.5	14.4

[a] Degree of polymerization. [b] Determined by gel permeation chromatography. [c] Calculated from the persistence length (6.5 nm) and the respective L_w according to eq 18.

In principle, this problem could be tackled by partial deuteration of the LPPP and a study of these materials solely by SANS. This rather tedious synthetic effort can be circumvented elegantly by the combined use of SANS and SAXS on the fully protonated LPPP. If solutions of the LPPP in a deuterated solvent are measured by SANS, the protonated alkyl side chains will give a strong scattering signal. On the other hand, the low number of excess electrons of the alkyl chains will lead only to a weak signal when conducting measurements by SAXS. As a consequence of this markedly different contrast within the repeating unit, the scattering behavior at high q is expected to be different for both types of radiation. This allows us to eliminate the effect of finite diameter of the chains. Both SAXS and SANS, however, must lead to the same result in the region of small scattering angles where the effect of finite chain diameter does not play a role. Going along these lines, the experimental scattering intensities can be evaluated to yield the form factor of the corresponding infinitely thin chain $P_0(q)$. This quantity can be compared to current theoretical treatments of wormlike chains to elucidate the spatial structure of the chains in solution.

Experimental Section

Toluene-d_8 (degree of deuteration = 99.95; Deutero GmbH) was used as received. The polymer LPPP has been synthesized as described previously.[1] The polymer was fractionated to yield three samples termed LPPP-24, LPPP-50, and LPPP-99. The fractionation was done using preparative gel chromatography (polystyrene gel; pore width; 10 000 Å; solvent; chloroform). The number-average molecular weight M_n (LPPP-24, M_n = 24 000; LPPP-50, M_n = 50 000; and LPPP-99, M_n = 99 000) and the polydispersities M_w/M_n of the samples (cf. Table 1) were estimated from an analysis by GPC using a polystyrene calibration (solvent: 1,2-dichloroethane).

The densities of the polymer solutions were determined using a DMA-60 apparatus supplied by Paar (Graz, Austria).

SANS Measurements. Small-angle neutron scattering has been performed on the D11 instrument of the Institut Laue-Langevin (ILL) in Grenoble using a wavelength of 0.6 nm. The range of scattering vectors was 0.032−1.5 nm^{-1} by using three different positions of the detector (2.5, 5, and 20 m). The protonated polymers were dissolved in deuterated toluene at concentrations ranging between 4.5 and 14 g/L. All data have been treated using the standard software supplied by the ILL.[15]

Absolute intensities at a detector distance of 2.5 m were obtained by normalizing the intensity scale by using the strong incoherent scattering of water as a standard. The absolute scattering cross section of H2O was calculated for the wavelength of 0.6 nm using the relation of Ragnetti et al.[16] Data deriving from measurements taken at different positions of the detector were normalized by using an appropriate factor determined from measurements of a Teflon probe.

The contribution $I_2(q)$ of the dissolved polymer was separated from the contribution of the solvent $I_1(q)$ by[11,12]

$$I_2(q) = I_{solution}(q) - (1 - \phi)I_1(q) \tag{1}$$

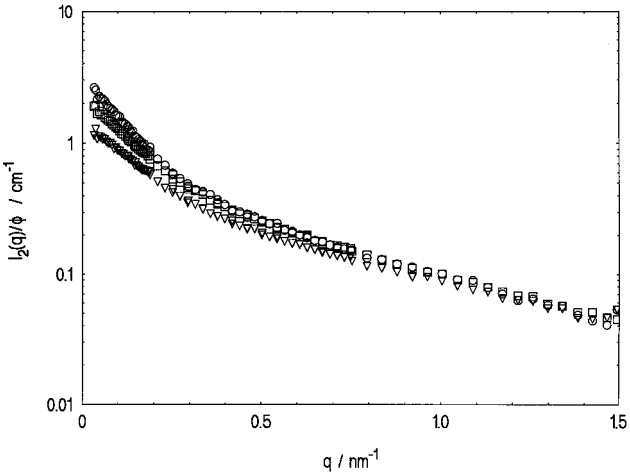

Figure 1. Absolute scattering intensities $I(q)$ (cf. eq 2) measured by SANS of polymer LPPP-99 for three different concentrations. All data have been normalized to weight concentration c: (○) c = 4.6 g/L; (□) c = 8.9 g/L; (▽) c = 13.5 g/L.

where ϕ is the volume fraction of the dissolved polymer. The small incoherent background due to the presence of the protonated polymers can be disregarded in good approximation.

The normalized intensity $I(q)$ of the dissolved polymers follows from $I_2(q)$ by

$$I_2(q) = cKI(q) \tag{2}$$

where c denotes the weight concentration of the polymer and K is the contrast factor defined by

$$K = \frac{\Delta b_{SANS}{}^2}{N_A} \tag{3}$$

N_A being Avogadro's number and Δb_{SANS} given by

$$\Delta b_{SANS} = b_2 - \rho_1 v_2 b_1 \tag{4}$$

Here b_1 and b_2 are the coherent scattering lengths[12] per unit mass of the solvent molecules and of the repeating units, respectively; v_2 is the partial specific volume of the polymer deduced from density measurements of the polymer solutions, and ρ_1 is the density of the solvent.

Figure 1 shows, as a representative example, the absolute scattering intensity $I_2(q)$ of LPPP-99 normalized to weight concentration according to eq 2. Within given limits of error the scattering intensities measured at different concentrations coincide at high q. At low q the scattering intensities decrease with increasing c as expected. The extrapolation to vanishing concentration can be done using the Zimm equation[12]

$$\frac{Kc}{I_2(q)} = \frac{1}{M_w P_z(q)} + 2A_2c + ... \tag{5}$$

where $P_z(q)$ is the z-average form factor of the polymer chains and A_2 is the second virial coefficient. Figure 2 displays a

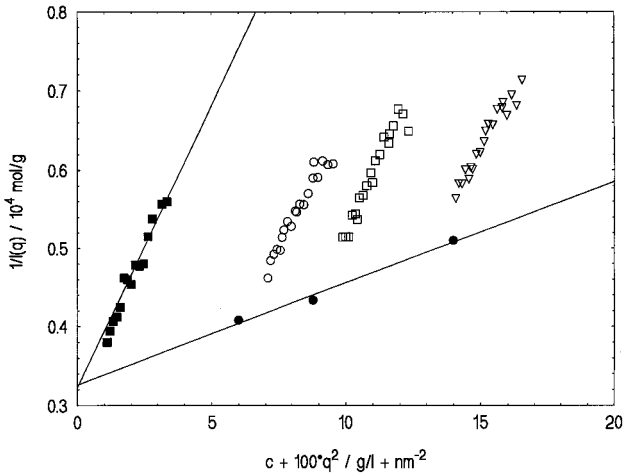

Figure 2. Zimm-plot of the intensities $I(q)$ (cf. eq 2) measured by SANS of polymer LPPP-24. For the sake of clarity only the extrapolations to $c = 0$ and $q = 0$ are displayed: (○) $c = 6.0$ g/L; (□) $c = 8.8$ g/L; (▽) $c = 14.0$ g/L.

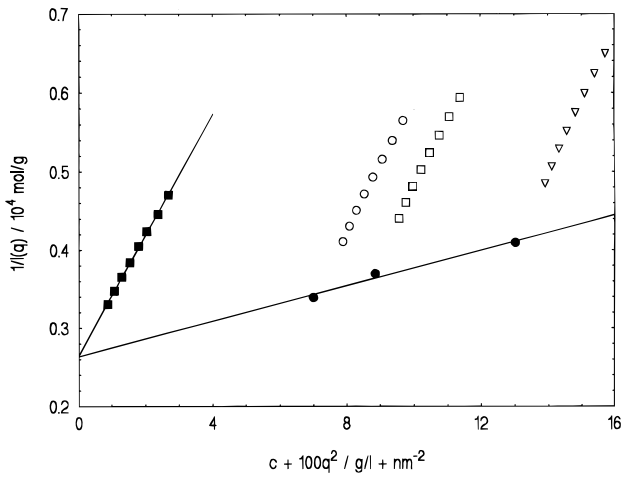

Figure 3. Zimm plot of the intensities $I(q)$ (cf. eq 2) measured by SAXS of polymer LPPP-50. For the sake of clarity only the extrapolations to $c = 0$ and $q = 0$ are displayed: (○) $c = 7.0$ g/L; (□) $c = 8.7$ g/L; (▽) $c = 13.0$ g/L.

Zimm plot obtained from SANS measurements of polymer LPPP-24. For the sake of clarity only the results of the respective extrapolations to vanishing concentration and to $q = 0$ are shown. Since there is no excess scattering in the range of low q, both extrapolations can be done without problems, giving the weight-average molecular weight M_w, the radius of gyration R_g, and the second virial coefficient with good accuracy. Table 1 gathers the data obtained by SANS from the three polymer samples.

In all cases discussed herein the extrapolation to vanishing concentration according to eq 5 had to be extended to rather high values of q. It turned out (see Figure 1) that the influence of interparticular interference, i.e., the influence of the structure factor, was still operative even at values of $qR_g \leq 5$. In all discussions to follow we only discuss normalized scattering intensities termed $I_0(q)$ extrapolated to $c = 0$ by application of eq 5.

SAXS Measurements: SAXS-measurements were done using a Kratky-Kompakt-Kamera (Paar, Graz, Austria) supplied with a position-sensitive counter (Braun, München, Germany). Details of measurements and evaluation of data have been given elsewhere.[17]

The calculation of absolute scattering intensities proceeds along the lines described for the SANS data above (cf. eqs 2−5). The quantity Δb_{SAXS} is calculated from Δz, the number of excess electrons per unit mass:

$$\Delta z = z - v_2 \rho_1 z_1 \tag{6}$$

where z_1 is the number of electrons per unit volume of the solvent. To ensure better comparison with the SANS data, all Δz have been multiplied by the Thomson factor[11] r_0 ($=2.8178 \times 10^{-13}$ cm) giving the absolute scattering amplitude of a single electron; i.e., $\Delta b_{SAXS} = \Delta z r_0$.

The extrapolation to vanishing concentrations is done by use of eq 5 to yield the normalized intensities $I_0(q)$ as discussed above. Figure 3 shows as an example the Zimm plot obtained from polymer LPPP-50. The data resulting from the SAXS measurements are collected in Table 1.

All Zimm plots obtained on the polymer LPPP do not show any sign pointing to association. The high value of A_2 which has been taken from SANS as well as from SAXS measurements shows that toluene is a good solvent for the LPPP and that the analysis is not disturbed by attractive interaction or by any kind of large undefined particles. This may be due to the fractionation procedure which turned out to be necessary in order to obtain meaningful results.

In this context it is interesting to compare the absolute scattering intensities $I_2(q)$ normalized to volume fraction. Figure 4 shows $I_2(q)/\phi$ obtained from sample LPPP-24 by SANS as well as by SAXS. It is immediately evident that both sets of data superimpose in the region of small angles where the

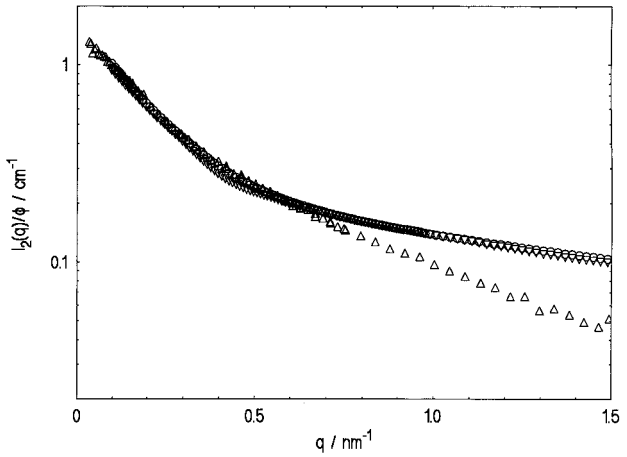

Figure 4. Comparison of the absolute scattering intensities $I_0(q)$ (extrapolated to $c = 0$) obtained from sample LPPP-50 using different radiation: SAXS (○; ▽; repetition of measurement) and SANS (△).

fine structure of the repeating unit does not show up, as discussed above. The good agreement of the SAXS and SANS data in this region as well as the good reproducibility (see SAXS data deriving from two different experiments in Figure 4) demonstrate the reliability of the measurements and the evaluation procedures. In particular, this agreement demonstrates that the absolute scattering intensities could be obtained with good accuracy despite the various errors which may be incurred when calculating the contrast factors according to eq 4 and 6.

At high q, however, both scattering curves deviate markedly. In this region the SANS data are decreasing much faster than the respective SAXS data. As already discussed in the Introduction, this points immediately to the strong influence of spatial structure of the repeating unit which allows us to distinguish between the effect of spatial extension of the chain and the finite diameter of its constitutive units.

Results and Discussion

Effect of Finite Diameter of the Repeating Unit. In general, the normalized scattering intensity $I_0(q)$ or the form factor $P_z(q)$ can be divided into three parts: (i) the region of low scattering angles (Zimm region) allowing us to determine the radius of gyration R_g (in this region the influence of concentration is most marked), (ii) the intermediate range where the scattering of flexible chains is governed by the excluded volume

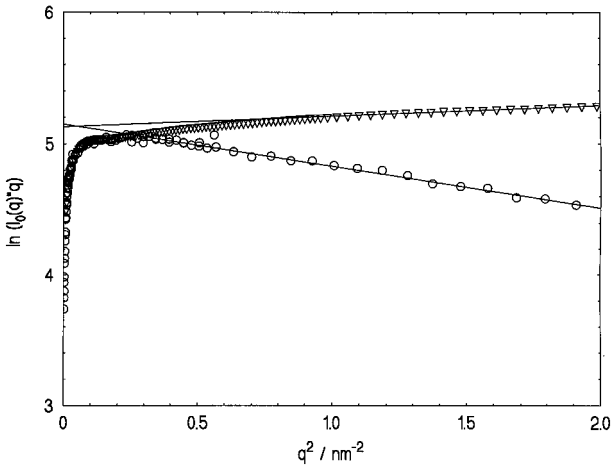

Figure 5. Determination of R_c by application of eq 10 to the data of LPPP-24; (▽) SAXS data; (○) SANS data.

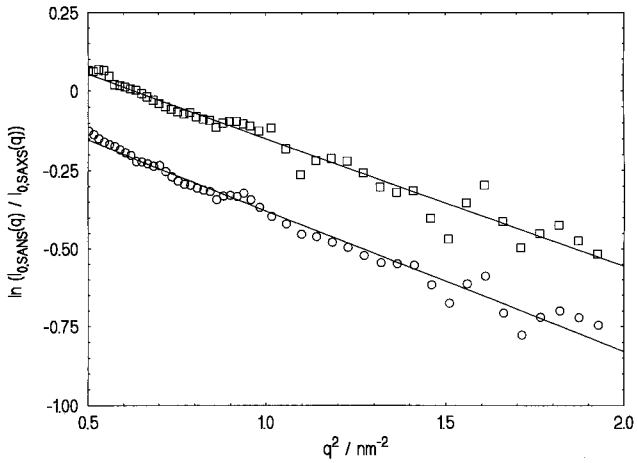

Figure 6. Check of the validity of eq 10: semilogarithmic plot of $I_{0,SANS}(q)/I_{0,SAXS}(q)$ of sample LPPP-24 (□) and of sample LPPP-50 (○).

exponent, and (iii) the region of high q where the interference is due to the short distance along the chain which may be regarded as rodlike (in this region there is no influence of the molecular nonuniformity).[12,13] Thus, in the classical model of the wormlike chain, the Kratky−Porod chain,[18−20] as well as in practically all other models[21−28] used up to now for calculating $P_0(q)$, the final slope is given by −1, i.e., $P_0(q)$ is proportional to q^{-1} at high q. This scaling law follows from the form factor of an infinitely thin needle of length L:[29]

$$P_0(q) = \frac{2}{qL}\left[\mathrm{Si}(qL) - \frac{1-\cos(qL)}{qL}\right] \tag{7}$$

where the sine integral is defined by

$$\mathrm{Si}(qL) = \int_0^{qL} \frac{\sin(x)}{x}\,\mathrm{d}x \tag{8}$$

For high q, eq 7 leads to

$$P_0(q) \rightarrow \frac{\pi}{qL} \tag{7'}$$

To account for the finite diameter the scattering intensity may be rendered as the product of a infinitely thin thread and a factor $\Phi(qR_c)$ ($\cong \exp(-1/2R_c^2q^2)$; cf. ref 21) describing the interferences due to the finite extension perpendicular to the long axis of the chain:[13,30]

$$I_0(q) = M_w P_0(qL)\Phi(qR_c) \tag{9}$$

where R_c denotes the radius of gyration perpendicular to the chain axis.

For $2\pi/L < q < 2\pi/R_c$, combination of (7′) and (9) leads to

$$I_0(q) \approx \frac{\pi M_L}{q}\exp\left[-\frac{1}{2}R_c^2q^2\right] \tag{10}$$

where M_L denotes the mass per unit length. Figure 5 shows the SANS and the SAXS data plotted according to eq 10. It is obvious that in both cases straight lines should result which have the same intercept. Figure 5 demonstrates that within experimental uncertainty the intercepts coincide. The slopes are different, however, as already expected from Figure 4. The resulting values of R_c^2 are given in Table 1. The small differences of the M_L derived from SAXS as compared to the ones determined by SANS (cf. Table 1) are mainly due to experimental uncertainties in the determination of absolute scattering intensities. Estimating the length of the repeating unit l_0 to 0.86 nm, M_L follows as 935 g/mol. This is in good agreement with the mean value 960 g/mol determined from SANS and SAXS. It underscores the validity of the above procedure.

The finding of a negative value of R_c^2 may be surprising at first. In order to test the above procedure to evaluate R_c^2 from the experimental data in another way, Figure 6 displays the logarithm of the ratio of the intensities $I_0(q)$ as obtained by SANS and by SAXS. The upper curve refers to the sample LPPP-24 whereas the lower curve displays the resulting data from sample LPPP-50. According to eq 10, the slope of this curve should be given by $R_{c,SANS}^2 + R_{c,SAXS}^2$. The respective value obtained experimentally is by 0.81 nm^2 for LPPP-50 and 0.89 nm^2 for LPPP-24 which compares favorably with the average value 0.85 nm^2 deduced from Figure 5. It is thus clear that eq 10 can be applied for both SANS and SAXS to obtain the contribution of $\Phi(qR_c)$ in both cases. Hence, eq 9 is fully applicable and the form factor of the corresponding infinitely thin thread can be obtained from the experimental scattering intensities $I_0(q)$.

The explanation of the negative values of R_c^2 rests in case of the SAXS measurements. Stuhrmann and Kirste[31] have been the first to show that the square of the radius of gyration R_g^2 can in principle assume positive and negative values. Following their arguments,[17,31,32] the quantity R_c^2 may be rendered as

$$R_c^2 = R_{c,\infty}^2 + \frac{\alpha\bar{\rho}}{\bar{\rho}-\rho_1} - \beta(\bar{\rho}-\rho_1)^{-2} \tag{11}$$

where $\bar{\rho}$ is the average scattering length density per area, $R_{c,\infty}^2$ is the value of R_c^2 at infinite contrast, and α presents the second moment of the internal electron density distribution. The contrast $(\bar{\rho}-\rho_1)$ is related to the excess scattering length per unit mass as defined by eq 4 through

$$r_0(\bar{\rho}-\rho_1) = \Delta b/\nu_2 \tag{12}$$

The contribution of the order $(\bar{\rho}-\rho_1)^{-2}$ relates to the dependence of the center of gravity on contrast. Equation 11 shows immediately that R_c^2 as well as R_g^2 must diverge directly at the match point. Both quantities will therefore show a most pronounced variation with con-

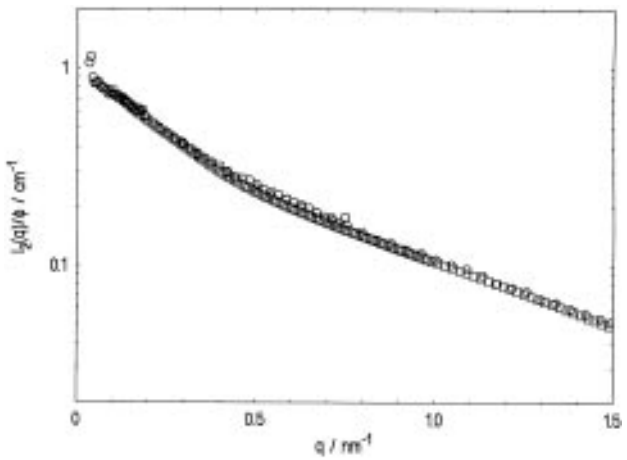

Figure 7. Check of the validity of eqs 9 and 10: Absolute normalized scattering intensities $I_0(q)$ obtained from LPPP-24 by SAXS (□) and by SANS (○) divided by $\Phi(qR_c)$.

trast around the match point. For a qualitative discussion of R_c^2 it suffices to discuss the sign of the coefficient α for SAXS and SANS; a more elaborate investigation of this point would require measurements at more than two different contrasts ($\bar{\rho} - \rho_1$).

The moieties possessing the highest electron densities, i.e., the phenyl groups, are located near the main axis of the chain, whereas the hydrocarbon chains protruding into the solvent have a lower excess electron density than the solvent toluene. Therefore in the case of the SAXS data α is negative (cf. the discussion of this quantity in ref 16). As a consequence, R_c^2 may become negative if the positive contrast ($\bar{\rho} - \rho_1$) is low enough.

In the case of SANS, the contrast as expressed by Δb_{SANS} ($=-5 \times 10^{10}$ cm^{-2}) is negative and considerably stronger than Δb_{SAXS} ($=1.5 \times 10^{10}$ cm^{-2}). As discussed above, the hydrocarbon chain containing a large number of hydrogen atoms will give the main scattering contribution in the case of SANS. The hydrogen atoms exhibit a more negative scattering length than the backbone of the chains. Therefore α will be negative. The solvent is characterized by a strongly positive b_1 (cf. eq 4) and ($\bar{\rho} - \rho_1$) is therefore negative. The contrast-dependent term in eq 11 is in consequence positive, as expected from the present experimental data. It is thus evident that the different values of R_c can be rationalized from the structure of the repeating units.

The above discussion has clearly revealed that the present combination of SANS and SAXS data allows us to determine the function $\Phi(qR_c)$ in an unambiguous manner. The reduced scattering intensities $M_wP_0(q)$ (see eq 9) obtained from different radiations should therefore coincide throughout the entire range of scattering vectors because they correspond to the scattering of an infinitely thin thread. Figure 7 shows that this is the case in very good approximation.

Form Factor $P_0(q)$ of an Infinitely Thin Chain. The data thus obtained now can be compared with current theoretical expressions for $P_0(q)$ of wormlike chains. Since the first publication of Kratky and Porod[18,19] in 1949 the calculation of $P_0(q)$ for wormlike chains is among the classical problems of polymer physics. The stiffness is measured by the persistence length termed a, which is half of the Kuhn length l_K. Most of the expressions are restricted to a certain ratio of the persistence length to the contour length L of the chains.[21] Thus, Yamakawa and Fujii[25] as well as Norisuye and co-workers[26] developed expressions for very stiff chains whereas Sharp and Bloomfield[33] worked out an expression for the limit of rather flexible chains, i.e., to be used at small a/L. An approximate theory comprising both limits has been worked out by Koyama[24] and extensively applied to experimental results by Burchard and co-workers[34−40] and by Shukla et al.[41] As shown by Huber et al.,[35] however, the Koyama form factor slightly underestimates $P_0(q)$ at higher q. Also, in this region it does not fully coincide with the expression given by Yamakawa and Fujii.[25]

Recently, Kholodenko[28] presented an entirely new approach using the analogy between Dirac's fermions and semiflexible polymers. The form factor $P_0(q)$ resulting from Kholodenko's approach is designed to reproduce correctly the rigid-rod limit (given by eq 7) and the random-coil limit. Defining $x = 3L/2a$, it is given by

$$P_0(q) = \frac{2}{x}\left[I_{(1)}(x) - \frac{1}{x}I_{(2)}(x)\right] \tag{13}$$

where

$$I_{(n)}(x) = \int_0^x f(z)z^{n-1}\,\mathrm{d}z \tag{14}$$

together with

$$f(z) = \frac{1}{E}\frac{\sinh(Ez)}{\sinh(z)} \qquad q \le \frac{3}{2a}$$

$$= \frac{1}{\hat{E}}\frac{\sin(\hat{E}z)}{\sinh(z)} \qquad q > \frac{3}{2a} \tag{15}$$

and

$$E = \left[1 - \left(\frac{2}{3}aq\right)^2\right]^{1/2} \qquad \hat{E} = \left[\left(\frac{2}{3}aq\right)^2 - 1\right]^{1/2} \tag{16}$$

The integrals in eq 14 can be conveniently obtained numerically, and eq 13 allows us to calculate the form factor of wormlike chains for all ratios of a to L. Model calculations showed that Kholodenko's expression practically coincides with $P_0(q)$ of stiff chains as furnished by Yamakawa and Fujii.[25]

To take into account the polydispersity of the samples, the z-average of the theoretical expressions $P_0(q)$ is calculated according to

$$P_{0,z}(q) = \frac{\int_0^\infty P_0(qL)w(L)L\,\mathrm{d}L}{\int_0^\infty w(L)L\,\mathrm{d}L} \tag{17}$$

where $w(L)$ is the weight fraction of the chains having the contour length L. In all subsequent calculations a Schulz−Zimm distribution has been used

$$w(L) = \frac{L^m}{\Gamma(m+1)}y^{m+1}\exp[-yL] \tag{18}$$

Here $y = (m + 1)/L_w$ where L_w is the weight-average contour length of the chains and m is a parameter characterizing the polydispersity of the chains [$m^{-1} = (L_w/L_n - 1)$].

The fit of eq 16 to the form factors $P_{0,z}(q)$ proceeded as follows: The persistence length a was determined by fitting eq 16 to the highest molecular weight LPPP-99. The contour length L_w necessary for this calculation follows directly from M_w as determined from the Zimm plots (see Figures 2 and 3) and the M_L values gathered

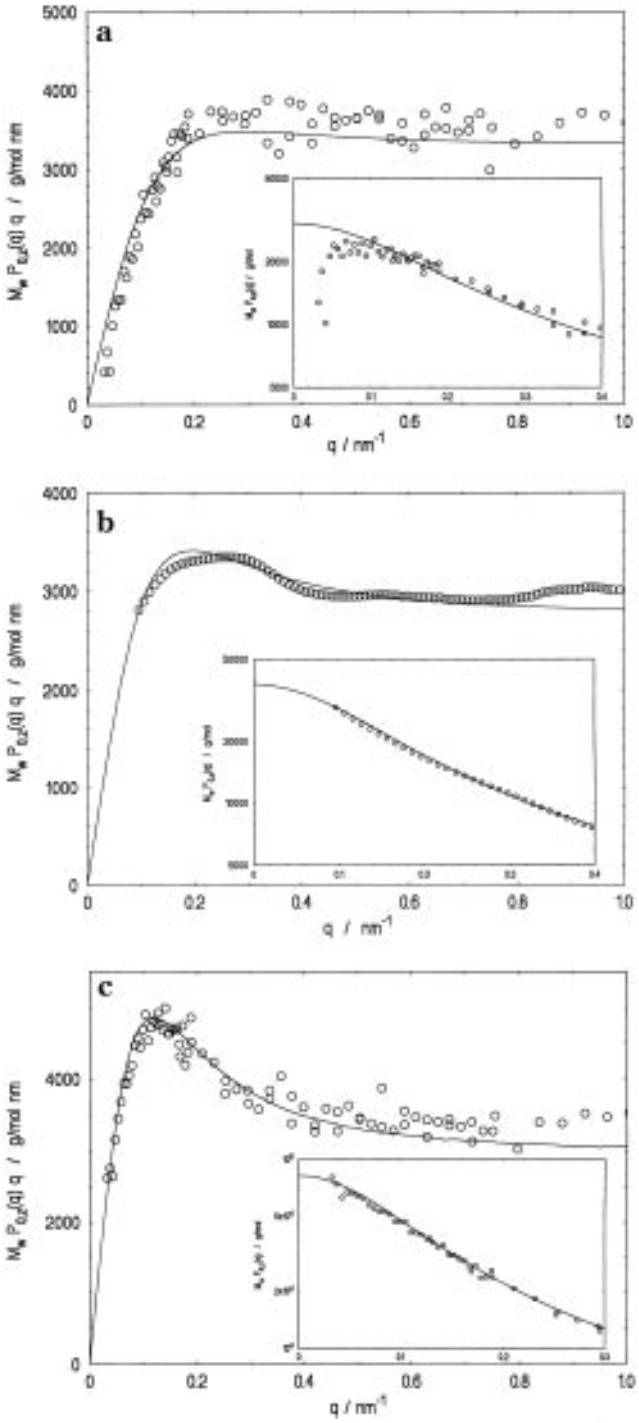

Figure 8. Comparison of the theoretical form factor $P_{0,z}(q)$ of a polydisperse, infinitely thin wormlike chain (ref 28; cf. eqs 13−17) with experimental data: (a) LPPP-24; (b) LPPP-50; (c) LPPP-99. For better comparison $P_{0,z}(q)$ has been multiplied by M_w; i.e., in all cases the plateau is given by πM_L (cf. eq 10). The insets display $P_{0,z}(q)M_w$ in the region of smallest angles.

in Table 1. The polydispersities (cf. Table 1) have been estimated from an analysis of the LPPP by gel permeation chromatography. The resulting persistence length of 6.5 nm was used to calculate directly the $P_{0,z}(q)$ of LPPP-50 and -24. The respective comparisons of the fits and the experimental data are given in Figure 8a−c. For better comparison between the different molecular weights, the normalized intensity $M_w P_{0,z}(q)$ of an infinitely thin chain is shown. Since $M_w P_{0,z}(q)$ will approach $\pi M_L/q$ at high q, the data displayed in Figure 8 have been multiplied by q. The insets show $M_w P_{0,z}(q)$ as a function of q in the region of small angles. Good agreement is seen in all three cases throughout the entire range of q; residual discrepancies are within given limits of error. Also, for all three molecular weights the $M_w P_{0,z}(q)$ data tend to the plateau given by $M_L\pi$ as predicted by eq (10).

The calculated form factors must also reproduce the radii of gyration R_g deduced from the Zimm plots (cf. Table 1). In contrast to the scattering data at high q, R_g is highly sensitive to the breadth of the molecular weight distribution. Table 1 gathers the z-average radii of gyration calculate according to[42]

$$R_{g,z}{}^2 = \frac{(m+2)a}{3y} - a^2 + \frac{2ya^3}{(m+1)} - \frac{2a^4}{m(m+1)}\left[y^2 - \frac{y^{m+2}}{\left(y+\frac{1}{a}\right)m}\right] \quad (19)$$

The comparison shows that a persistence length of approximately 6.5 nm is in good agreement with the experimental data.

In principle, the expression for R_g furnished by Kholodenko[28] could be used as well to calculate the z-average $R_{g,z}{}^2$ instead of using eq 18. Calculations showed, however, that the differences between the two expressions are marginal for the present range of a/L and within experimental uncertainty.

The rather high persistence justifies now the neglect of the excluded volume effect in the above treatment: Even in case of the highest molecular weight LPPP-99 the chains embody only ca. 7 Kuhn segments. Tsuboi et al.,[43] however, could show recently that excluded volume effects become experimentally observable if the number n_K of Kuhn segments exceeds 50. The much smaller n_K characterizing the LPPP therefore leads to the conclusion that this effect can be safely dismissed in the course of the present study.

Conclusion

The analysis of the ribbon-type polymers under consideration here has clearly shown that these polymers must be regarded as wormlike chains despite their all-aromatic structure consisting of stiff, collinear repeating units. In agreement with previous findings[6−10] obtained on similar systems and with recent computer simulations[44−46] this demonstrates that bending fluctuations will destroy the rodlike structure and lead to a wormlike shape of the chains even when the repeating unit is built up from stiff moieties. The effect of bending fluctuations will be enhanced by the bulky substituent R_2 which may distort the linear shape of the repeating unit as well.

The same argument immediately leads to the conclusions that such bending fluctuations will prevent a two-dimensional structure of the ribbons: On the one hand, due to the molecular structure, fluctuations out of the plane of the ribbons will occur much more often than torsional fluctuations of the repeating units. On the other hand, even a minute torsion per repeating unit of the order of 1−2° will lead to an overall three-dimensional structure for chains with degree of polymerization greater than 20−30. As a consequence, the LPPP exhibit a three-dimensional spatial structure in agreement with the above analysis.

Acknowledgment. Financial support by the Deutsche Forschungsgemeinschaft and by the Bundesmin-

isterium für Bildung und Forschung is gratefully acknowledged.

References and Notes

(1) Scherf, U.; Müllen, K. *Makromol. Chem. Rapid Commun.* **1991**, *12*, 489.
(2) Scherf, U.; Müllen, K. *Adv. Polym. Sci.* **1995**, *123*, 1.
(3) Leising, G.; Grem, G.; Leditzky, G.; Scherf, U. *Proc. SPIE* **1993**, *1910*, 70.
(4) Grüner, J. F.; Hamer, P.; Friend, R. H.; Huber, J.; Scherf, U.; Holmes, A. B. *Adv. Mater.* **1994**, *6*, 748.
(5) Scherf, U.; Bohnen, A.; Müllen, K. *Makromol. Chem.* **1992**, *193*, 1127.
(6) Galda, P.; Kistner, D.; Martin, A.; Ballauff, M. *Macromolecules* **1993**, *26*, 1595.
(7) Tiesler, U.; Pulina, T.; Rehahn, M.; Ballauff, M. *Mol. Cryst. Liq. Cryst.* **1994**, *243*, 299.
(8) Schmitz, L.; Ballauff, M. *Polymer* **1995**, *36*, 879.
(9) Tiesler, U.; Schmitz, L.; Ballauff, M. *Mol. Cryst. Liq. Cryst.* **1994**, *254*, 387.
(10) Tiesler, U.; Rehahn, M.; Ballauff, M.; Petekidis, G.; Vlassopoulos, D.; Maret, G.; Kramer, H. *Macromolecules*, in press.
(11) Glatter, O., Kratky, O., Eds. *Small Angle X-Ray Scattering;* Academic Press: London, 1982.
(12) Huggins, J. S.; Benoit, H. C. *Polymers and Neutron Scattering;* Clarendon Press, Oxford, U.K., 1994.
(13) Rawiso, M.; Duplessix, R.; Picot, C. *Macromolecules* **1987**, *20*, 630.
(14) März, K.; Lindner, P.; Urban, G.; Kugler, J.; Ballauff, M.; Fischer, E. W. *Acta Polym.* **1993**, *44*, 139.
(15) Ghosh, R. E. *Computing Guide for Small Angle Scattering Experiments*; ILL Technical Report 896H02T; Institute Laue-Langevin: Grenoble, France, 1989.
(16) Ragnetti, M.; Geiser, D.; Höcker, H.; Oberthür, R. C. *Makromol. Chem.* **1985**, *186*, 1701.
(17) Hickl, P.; Ballauff, M.; Jada, A. *Macromolecules* **1996**, *29*, 4006. Ballauff, M.; Bolze, J.; Dingenouts, N.; Hickl, P.; Pötschke, D. *Macromol. Chem. Phys.* **1996**, *197*, 3043.
(18) Porod, G. *Monatsh. Chem.* **1949**, *80*, 251.
(19) Kratky, O.; Porod, G. *Recl. Trav. Chim.* **1949**, *68*, 1106.
(20) Flory, P. J. *Statistical Mechanics of Chain Molecules,* 2nd ed.; Hanser Publishers: Munich, 1989.
(21) Oberthür, R.; Kirste, R. G. In *Small Angle X-Ray Scattering;* Glatter, O.; Kratky, O., Eds.; Academic Press: London, 1982; Chapter 12.
(22) Hermans, J. J.; Ullman, R. *Physica* **1952**, *18*, 951.
(23) Hermans, J.; Hermans, J. J. *J. Phys. Chem.* **1958**, *62*, 1543.
(24) Koyama, R. *J. Phys. Soc. Jpn.* **1973**, *34*, 1029.
(25) Yamakawa, H.; Fujii, M. *Macromolecules* **1974**, *7*, 649.
(26) Norisuye, T.; Murakama, H.; Fujita, H. *Macromolecules* **1978**, *11*, 966.
(27) Hammouda, B.; Garcia Molina, J. J.; Garcia de la Torre, J. *J. Chem. Phys.* **1986**, *85*, 4120.
(28) Kholodenko, A. L. *Macromolecules* **1993**, *26*, 4179.
(29) Neugebauer, T. *Ann. Phys.* **1943**, *42*, 509.
(30) Koyama, R. *J. Phys. Soc. Jpn.* **1974**, *36*, 1409.
(31) Stuhrmann, H. B.; Kirste, R. G. *Zr. Phys. Chem. N. F.* **1967**, *56*, 334.
(32) Feigin, L. A.; Sholer, I. *Sov. Phys. Crystallogr.* **1975**, *20*, 302. Cf. als: Hickl, P.; Ballauff, M. *Physica A*, in press.
(33) Sharp, P.; Bloomfield, V. *Biopolymers* **1968**, *6*, 1201. See correct expression in ref 20.
(34) Schmidt, M.; Paradossi, G.; Burchard, W. *Makromol Chem. Rapid Commun.* **1985**, *6*, 767.
(35) Huber, K.; Burchard, W.; Bantle, S. *Polymer* **1987**, *28*, 863.
(36) Dentini, M.; Coviello, T.; Burchard, W.; Crescenzi, V. *Macromolecules* **1988**, *21*, 3312.
(37) Burchard, W. *Makromol. Chem. Macromol. Symp.* **1988**, *18*, 1.
(38) Denkinger, P.; Burchard, W. *J. Polym. Sci., Polym. Phys. Ed.* **1991**, *29*, 589.
(39) Lang, P.; Kajiwara, K.; Burchard, W. *Macromolecules* **1993**, *26*, 3992.
(40) Lang, P.; Burchard, W. *Makromol. Chem.* **1993**, *194*, 3157.
(41) Shukla, P.; Cotts, P. M.; Miller, R. D.; Russell, T. P.; Smith, B. A.; Wallraff, G. M.; Baier, M.; Thiyagarajan, P. *Macromolecules* **1991**, *24*, 5606.
(42) Schmidt, M. *Macromolecules* **1984**, *17*, 553.
(43) Tsuboi, A.; Norisuye, T.; Teramoto, A. *Macromolecules* **1996**, *29*, 3597.
(44) Jung, B.; Schürmann, B. *Macromolecules* **1989**, *22*, 477.
(45) Jung, B.; Schürmann, B. *Macromolecules* **1992**, *25*, 1003.
(46) Farmer, B. L.; Chapman, B. R.; Dudis, D. S.; Adams, W. W. *Polymer* **1993**, *34*, 1588.

MA961038S